Thirteenth USA/Europe Air Traffic Management Research and Development Seminar (ATM2019)

Time-Based Delivery Accuracy Requirements for Achieving Performance Based Navigation Objectives

Matthew R. Pollock, Dr. Lesley A. Weitz, Dr. Jared A. Hicks, and John M. Timberlake
Center for Advanced Aviation System Development (CAASD)
The MITRE Corporation
McLean, Virginia
mpollock@mitre.org

***Abstract*—Trajectory Based Operations relies on managing aircraft according to a schedule while keeping aircraft on defined and planned arrival paths to the runway. This work uses simulation data to investigate the delivery accuracy requirements needed in a metering operation to support target rates of aircraft remaining on their planned routes.**

Keywords: TBO; TBM; PBN; simulation; performance requirements

I. INTRODUCTION

Trajectory Based Operations (TBO) combines Time-Based Management (TBM) operations and Performance-based Navigation (PBN) to improve the predictability and efficiency of air traffic operations [1]. To achieve TBO benefits, TBM operations and PBN procedures must be designed to enable flights to remain on their planned routes throughout the arrival and approach phases of flight [2].

TBM operations involve the use of the Time-based Flow Management (TBFM) system, which is an Air Traffic Control (ATC) decision support system used to develop a sequence and schedule of aircraft down to the runway, deconflicting flights at key points in the airspace by determining Scheduled Times of Arrival (STAs) at Meter Reference Points (MRPs) [3]. If two flights are predicted to cross an MRP with insufficient spacing, the trailing aircraft's STA will be delayed providing the minimum required spacing, and that aircraft will need to fly a longer flight time to the MRP [4]. If the required flight time is too long and the delay cannot be absorbed using a slower speed alone, ATC may need to lengthen the aircraft's path to the MRP to meet the STA. Additionally, when ATC is managing flights to their STAs, tactical interventions may be needed to ensure separation between flights resulting from delivery errors of preceding flights to their STAs.

PBN procedures define a three-dimensional path through the airspace. The route of flight over the ground is defined using waypoints, and the vertical flight path may be constrained at waypoints using precise altitude constraints or altitude windows. PBN procedures can be designed to deconflict arrival and departure flights or procedures to different airports. Speed constraints may also be added to waypoints to provide greater predictability and reduce the chance of compression issues (i.e., spacing between flights reducing as they slow down).

The future TBO environment will enable time-based metering for arrival and approach operations, starting in en route airspace. Arrival and approach operations will be divided into smaller distances, over which flight-time predictions and schedules are more accurate, using MRPs. Aircraft flows into constrained airspace, such as high-density terminal environments, will be pre-conditioned starting several hundred miles from the terminal airspace, allowing the use of speed control instead of vectoring to meet schedule times. Metering in en route airspace will involve Extended Meter Points (XMPs), Coupled Meter Points (CMPs), and the Meter Fix (MF) at the en-route/terminal boundary to precondition flows into the terminal [5]. In terminal airspace, the Terminal Sequencing and Spacing (TSAS) tools will support ATC in managing aircraft to their STAs at Terminal Meter Points (TMPs) [6] [7] [8]. The placement of TMPs supports ATC in merging flows and managing a mixed-equipage environment, where some aircraft are equipped with Required Navigation Performance (RNP) avionics, allowing those flights to fly shorter RNP approach procedures to the runway than unequipped flights.

To maximize PBN benefits, the relationship between TBM performance (i.e., the accuracy with which aircraft meet their STAs at MRPs) and PBN benefits (i.e., the percentage of flights that remain on their planned routes throughout the arrival and approach operation, thus benefitting from more efficient routes) must be understood. This relationship is dependent on operational characteristics, such as the number of arrival runways, runway demand, and the use of Required Navigation Performance (RNP) approach procedures, design of the Standard Terminal Arrival (STAR) as well as the interactions of merging flows and traffic densities or flow rates at different points in the airspace. The objective of this work was to develop a mathematical model for TBM operations that reflects the complex relationships between operational characteristics, performance requirements, and PBN objectives. This model was developed using results from fast-time simulations, which reveal the complex relationships between the schedule and the execution of that schedule given different TBM and PBN designs. While previous analyses have related TBM performance and PBN conformance [9] [10] [11], those analyses either failed to capture operational complexities or were operationally-specific and results are not easily extensible to other TBM sites and operational characteristics.

In this work, a fast-time simulation model of TBM operations was developed to determine the relationship between operational characteristics, TBM performance, and PBN benefits. The fast-time simulation is a discrete-event model, which is driven by a weighted graph that represents a TBM operation and the airspace. The remainder of the paper is organized as follows. The fast-time simulation model is described in Section II. The simulation experiment design and validation of the fast-time simulation are described in Sections III and IV, respectively. Results from the fast-time simulation are presented in Section V, and lastly, conclusions are provided in Section VI.

II. Fast-Time Simulation Model

In the fast-time simulation, the TBM operation, or metering operation, was modeled at discrete points in time when an aircraft crossed one of the defined locations known to the model (a graph node in the discussion below), causing a change in the state of the system. Between events, there is no change in the system state, and time advances in jumps from one event time to the next.

The model represents operations using a directed weighted graph, where sequences of nodes and edges represent routes that aircraft may traverse between points in the airspace. This is illustrated in Figure 1, which shows a simple directed weighted graph with potential routes from initial locations to destinations (i.e., parallel runways). Notional traversal time ranges and probabilities are given for each edge. The traversal time ranges refer to the variability in observed flight times between these points in the airspace. Probabilities equal to 1.0 mean flights traversing the upstream node will always go to the downstream node. However, in those cases where upstream nodes are connected to two or more downstream nodes, the flight may be routed along any one of those edges. Route selection is designed to pick the most likely route.

The nodes in the directed weighted graph represent locations where discrete events may occur; i.e., the state of the system is evaluated and changed when flights reach nodes. The nodes may be assigned attributes. For example, some nodes are MRPs or freeze horizons. Two of the nodes in Figure 1 are labeled as freeze horizons (coinciding with the dashed lines). When a flight reaches a freeze-horizon node, the TBFM schedule is updated based on the state of the system and that flight's schedule is frozen at all downstream MRPs associated with that freeze horizon. The system state includes frozen STAs for flights that have already crossed the freeze horizon, as well as the estimated times of arrival (ETAs) describing when flights upstream of the freeze horizon are expected to cross downstream scheduling nodes.

There are four main components to the model used in combination to represent TBM operations:

- **Traffic Management Coordinator (TMC)**: the TMC is responsible for assigning flights to routes from their origins to their destinations. In a TBM operation, the assigned routes are based on coordinating with the TBFM Scheduler.

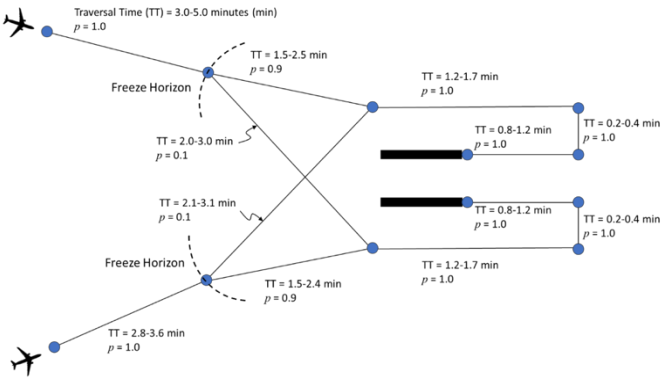

Figure 1. Directed Weighted Graph Example with Nodes and Edges Shown with Notional Traversal Times and Probabilities for each Edge

- **TBFM Scheduler**: the emulation of the TBFM scheduler determines STAs at MRPs based on ETAs to those points and any delays needed to deconflict flights at MRPs.
- **Flight Model**: flights progress through the weighted graph based on traversal time distributions. Planned traversal times are adjusted to meet STAs or for tactical controller intervention to prevent conflicts.
- **Controller Model**: the controller model monitors separation at all nodes and intervenes as needed to prevent conflicts. Strategic intervention distributes TBFM-planned delay upstream of MRPs. Tactical interventions at a downstream node (MRP or otherwise) are modeled by increasing the traversal times along the preceding edge. However, if insufficient delay authority is available, tactical reroutes are also possible.

In summary, the TMC and TBFM Scheduler components model the TBFM components that determine the arrival plan, and the flight and controller models represent the execution to the arrival plan.

III. Simulation Design

A. Model Configurations

Since PBN utilization is an output of the simulation, the simulation inputs fall into two categories: (1) operational characteristics and (2) STA meet-time performance. The following variables reflect the operational characteristics:

Weather: The model was run in both Instrument Meteorological Conditions (IMC) and Visual Meteorological Conditions (VMC). The weather input corresponded with a weather-specific TBFM configuration at Denver International Airport (KDEN). The primary differences between the simulation in IMC mode and the simulation in VMC mode are the scheduling mode (to the runway or final approach fix), separation matrices, and downwind leg length.

STARs per Corner Post: KDEN operates with dual STARs, meaning each corner post (NE, SE, SW, and NW) is served by two separate arrival procedures. A more typical arrangement is to have one STAR per corner post (assuming a four-corner post design). Validation was conducted using dual STARs and

experimental simulations were run both for dual STARs and a single STAR per corner post.

Number of Runways: Simulations were conducted using one, two, and three independent arrival runways. In the two- and three-runway case, RNP approaches were available to the outboard runways (34R on the west side of the airport and 35R on the east side). RNP approaches needed to be prototyped for the one-runway configuration since they do not exist in the suite of published KDEN approaches. Figure 2 illustrates how RNP approaches were mapped to runway configurations.

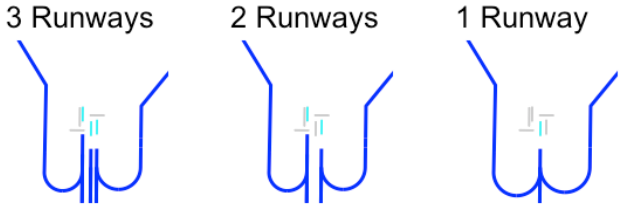

Figure 2. Simulated Runway Configurations

RNP Equipage: Although mixed-equipage scenarios are an interesting topic pertinent to all operations with RNP approach procedures, this analysis was scoped to consider only the two extreme cases: (1) operations with zero RNP equipage (or equivalently, operations without RNP approaches) and (2) operations with 100-percent RNP equipage. Mixed-equipage scenarios were considered only for the validation scenarios to represent current operations at KDEN.

Arrival Demand: Demand was measured in aircraft per hour per runway. Thus, a rate of 15 would mean 15 aircraft per hour in a one runway simulation, but 45 aircraft per hour in a three-runway simulation.

The second simulation input is the *delivery error* at different MRPs. Delivery error is modeled using a standard deviation of a (truncated) normal distribution with mean zero. In the degenerate case of a zero-value standard deviation, there is no delivery error and perfect delivery accuracy is assumed. As the standard deviation of this distribution is increased, the delivery accuracy deteriorates, and delivery errors are larger. Since errors are governed by a normal distribution, a reasonable rule of thumb is to double the standard deviation to arrive at a delivery accuracy target. This covers about 95% of errors. For example, if the error standard deviation is 30 seconds (s), then we would expect simulation controllers to deliver aircraft within ±1 minute (min) of the STA.

Four different delivery errors were used for each simulation. One for delivering aircraft to the XMP, which is farthest from the airport (tested with settings of 0 s and 5 min); one for delivering aircraft to the CMP, which is a little closer (testing 0 s, 90 s, and 3 min); one for delivering aircraft to the Meter Fix (MF) at the Terminal Radar Approach Control (TRACON) boundary (testing 0 s to 60 s in 15 s increments); and one for use at the deconfliction points inside the TRACON (using TSAS, testing 0 s to 24 s in 6 s increments). These MRPs are depicted in Figure 3, which shows the simulation input graph. To simplify and genericize the simulation, XMP and CMP arcs were placed 350 NM and 200 NM from the airport reference point, respectively. Freeze horizons were 150 NM from the MRPs.

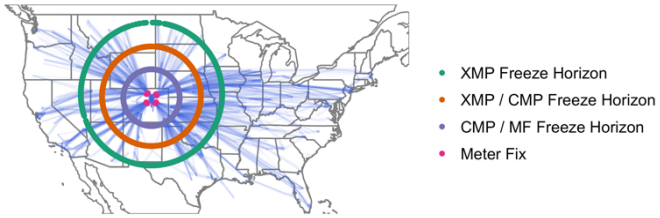

Figure 3. Input Graph with Labeled MRPs

Using the rule of thumb stated above, the worst-case scenario assumes the following 95% delivery errors: ±10 minutes at the XMP, ±6 minutes at the CMP, ±2 minutes at the MF, and ±48 seconds inside the TRACON. In total, 150 different combinations of MRP delivery errors were considered.

For TBFM, internal departures are those originating from airports inside the metering operation. In this case, inside the XMP freeze horizon. These flights are immediately frozen in the schedule when they depart and therefore sometimes need to take delay on the ground. Since the flight miles between departure and the next MRP is, by definition, shorter for internal departures than for other flights (which are frozen at the freeze horizon), precision in departure time to help absorb delay to the MRP is critical. In this model, the internal departure release time precision was not an input. Instead, it was assumed departure controllers would meet the call for release compliance window in all cases (such that the MRP ETA falls between 2 min early to 1 min late). In cases where the ETA falls within the window it is unchanged. In cases where the ETA is more than 2 min early, then ground delay is taken such that the release time error falls anywhere in the interval (following a uniform distribution). Once the flight departs, the simulated controller adjusts the flight's traversal time as needed to compensate for imprecise departure times and meet the STA at the MRP within the specified delivery error.

B. *Performance Metrics*

Several metrics were collected in the simulation results, including runway throughput (actual and planned), delay (airborne and ground), and actual delivery error (to check inputs). However, the primary output is the fixed path rate. Flights that flew fixed paths were those that (1) stayed on their planned route and (2) had a delay rate less than or equal to 10 percent of flight time along the route (i.e., at most six seconds of every minute flown while traversing the route is time added due to controller-directed delay).

C. *Airport Selection*

KDEN was selected as the simulation airport for this analysis because it contains airport and operational characteristics that may be viewed as a superset of those observed at many other National Airspace System (NAS) airports. As such, KDEN can be made to "look" and operate like other sites though partial selection and usage of these characteristics. For example, KDEN operates with dual STARs, but simulations can be configured to use only one STAR per corner post. Similarly, simulations can be conducted using one,

Sponsored by The Federal Aviation Administration

two, and three independent parallel arrival runways as shown in Figure 1. Varying these two characteristics allows simulations of KDEN to operate like a variety of other airports.

Figure 4 shows an example of KDEN configured to use a single STAR per corner post and three independent runways. These operational characteristics are similar to those often observed at Hartsfield-Jackson Atlanta International Airport (KATL), Dallas-Fort Worth International Airport (KDFW), and Chicago O'Hare International Airport (KORD). If dual STARs were used instead, the configuration would be more like Houston Intercontinental Airport's (KIAH) West configuration (dual STARs from NE/NW).

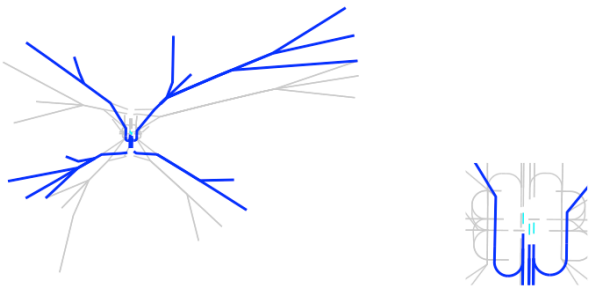

Figure 4. Example of KDEN Configuration Versatility (Three Runway Independent Operation)

Using selected versions of KDEN as proxies for airports not directly simulated allows for estimates of performance requirements at those airports. This is achieved by simulating KDEN under a wide variety of characteristics and fitting a statistical regression model to the simulation results.

IV. Fast-Time Simulation Validation

To validate the fast-time model, simulated traffic was generated using input configurations that mimic actual KDEN operations. This traffic was then compared to empirical data. This exercise ensured the model appropriately represents metering operations at KDEN by establishing the simulation produces results similar to those empirically observed when configured similarly to the real operation. This improves trust in the model output in cases for which empirical data does not exist. Exact matches are not expected. Exact matches may indicate overfitting of the model to specific inputs; however, overfitting may result in poorer predictions for other inputs. Rather, the objective is to have simulated output similar to, not exactly the same as, its empirical counterpart.

To configure the simulation to be like current KDEN operations, TSAS, extended metering, and coupled scheduling were all disabled, limiting the metering operation to the MFs at the TRACON boundary. KDEN-configured values for the TRACON buffer, route maximum delay (RMD)[1], and the TBFM-adapted routes were used in lieu of TSAS logic.

Since TSAS was disabled, STAs inside the TRACON (e.g., at the runway) were not visible to the simulation controllers. This is consistent with the current KDEN operation where the TBFM-planned sequence is not visible to TRACON controllers (except the TMC). One dissimilarity between the real KDEN operation and the simulation is that even with the runway STAs masked, the model remained deferential to TBFM with respect to runway assignments.

Since this study is scoped to consider only operations with independent arrival runways, KDEN south-flow operations were not eligible for consideration due to the spacing between runways 16R and 16L, which requires dependent arrivals. When in a north-flow operation, KDEN primarily operates with three runways: 34R, 35L, and 35R. Therefore, only the "N_IFR3A" and "N_VFR3A" TBFM configurations were considered. Given this choice of runway configurations and the dual-STARs design used at KDEN, the dual-STAR, three-runway input graph was used for validation simulations.

Validation scenarios were developed directly from observed traffic during periods when KDEN was operating in one of the two TBFM configurations of interest. This reuse of historical operations as recorded in the data (with respect to TRACON entry) differs from the random sampling scheme used for experimental simulations.

The demand was designed to match the actual KDEN demand at the time. Figure 5 shows the actual demand values that were simulated, ranging from fewer than 20 arrivals per hour to more than 60 arrivals per hour. Since the simulation did not support turboprop aircraft types, all turboprop aircraft in the validation scenario were replaced with randomly-selected jet aircraft types to retain the observed demand level.

RNP Authorization Required (AR) eligibility rates were estimated using the carrier and aircraft type of arriving aircraft. The distribution of estimated equipage rates is given in the left panel of Figure 6. Since there are a few surprisingly high and low values in the histogram, a scatter plot is included in the right panel to illustrate that the equipage rates are highly variable in scenarios with a small number of aircraft. However, in simulations with a larger number of aircraft, the equipage rates stabilize with a mean value just under 50%.

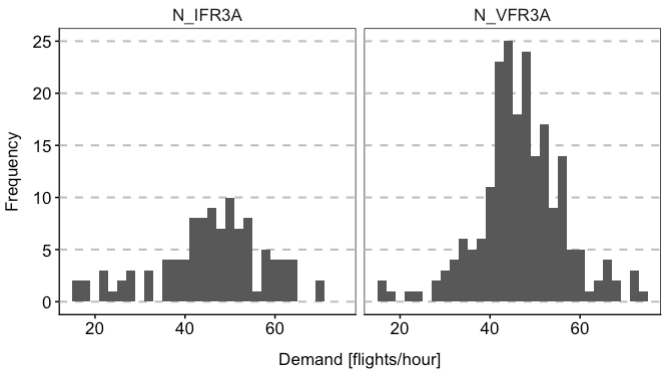

Figure 5. Historical Distribution of Demand at KDEN

[1] The RMD and TRACON buffer values are TBFM adaptation parameters. The RMD value defines the maximum delay for a given route, and the TRACON buffer defines a maximum amount of delay that can be taken in the TRACON for all routes. Because some routes may be shorter, the RMD value provides a more conservative bound on the delay for those routes.

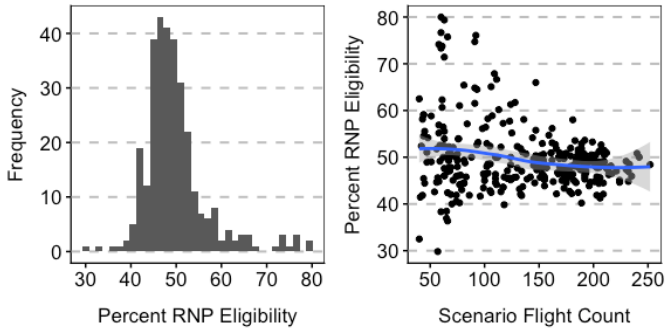

Figure 6. Historical RNP Eligibility Rates at KDEN

The final configuration necessary for validation was to determine the MF delivery error. Delivery errors within the TRACON and at the XMPs/CMPs were not necessary since STAs were only generated at the MF and runway for validation simulation runs. Using STAs and MF crossing times from the TBFM inter-process communications data, MF delivery errors were computed for arrivals during periods of TBFM being active. The standard deviation of these errors was found to be 1.42 min, which was used in the simulation.

A. PBN Utiliation Rates

In this work, PBN utilization is defined by three categories: (1) conformance to a STAR, (2) conformance to an RNP approach, and (3) conformance to an adapted fixed path approach.

Figure 7 shows the agreement between real and simulated operations was quite good (i.e., the medians and ranges of the distributions were similar) with respect to the percentage of arrivals that were able to conform well to one of the published KDEN STARs. Empirical arrivals were categorized as having flown a STAR if they adhered laterally (i.e., within 1 NM conformance bounds for RNAV) to at least 30% of the published procedure ground track.

Validation scenarios were designed with RNP equipage rates based on KDEN traffic. RNP approach utilization was then measured from the simulated operations. As Figure 8 shows, fewer RNP approaches were identified in the historical data than were supported in validation simulations. One reason for this is although Established on RNP (EoR) operations are conducted at KDEN [12] [13], they were suspended most of the date range used in this work pending a redesign of their RNP AR approaches. Given the simulated operations were using EoR-based separation rules while the empirical KDEN operation was not, observing fewer than double the number of RNP approach operations in the simulation when compared to the empirical operation was considered reasonable.

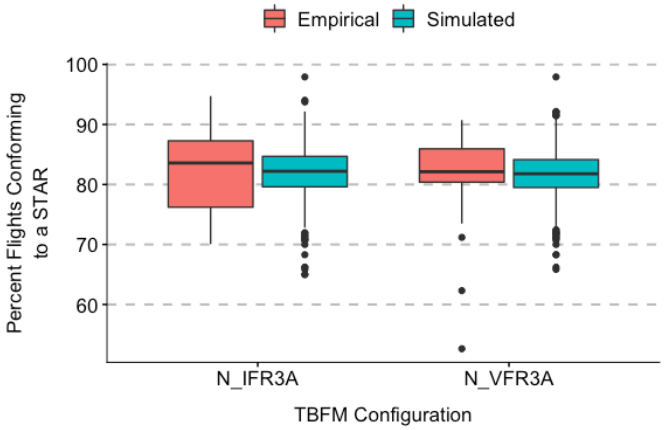

Figure 7. Simulated and Empirical STAR Utilization

B. Other Validation Metrics

Agreement between simulated output and empirical data was also checked relative to runway utilization, inter-arrival time (at both meter fixes and runways), throughput, and TRACON flight time. Like the PBN utilization results, these comparisons showed favorable matches.

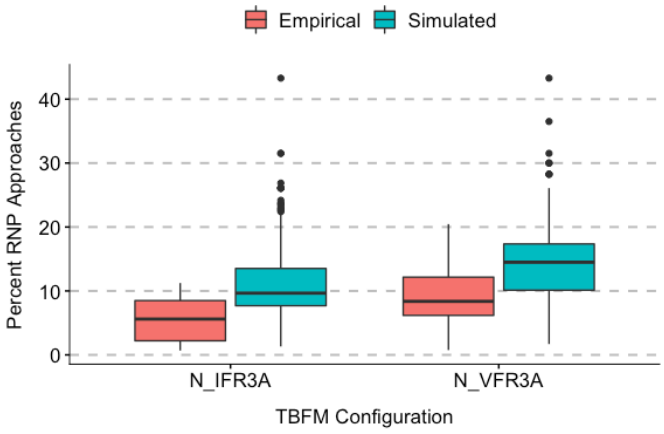

Figure 8. Simulated and Empirical RNP Approach Utilization

V. RESULTS

The objective of the experiment runs was to quantify the relationships between the PBN objective to keep aircraft on their planned routes, operational characteristics, and delivery errors. As such, the model was parameterized using two weather conditions (IMC and VMC), two STAR designs (single and dual STARs per corner post), three runway configurations (one runway, two independent runways, and three independent runways), eight demand values (15 flights per hour per runway up to 50 flights per hour per runway, in 5 flight increments), two RNP equipage settings (zero and 100 percent equipped), and 150 delivery error settings (crossing errors at the XMP, CMP, MF, and inside the TRACON)

Noting that dual-STAR designs were not considered in the one-runway scenarios, there are a total of 24,000 unique input

combinations. Each combination of inputs was simulated three times to account for random variability and generate enough data to support regression analysis of the results. Therefore, there were 72,000 possible simulation runs. Due to time constraints, data from a random sample of 61,600 simulations was available for this analysis. Each simulation represents 90 minutes of traffic, where the total number of operations is based on the runway demand (defined as demand per runway per hour) and the number of runways. Thus, for the low-demand case (one runway and 15 flights/runway/hour), 23 aircraft were simulated over the 90-minute block. For the high-demand case (three runways and 50 flights/runway/hour), 375 aircraft were simulated over the same time period.

Figure 9 provides a high-level summary of how each of the nine inputs influenced the percent of aircraft flying a fixed path. The violin plots in the figure show the relative concentration of data using the width of the blue and the 25th, 50th (median), and 75th percentile values using horizontal grey bars. One key take-away is that the most influential input is the runway demand, as indicated by discernable downward trend in the violin plots as a function of increasing runway demand. As demand on each runway increases, more aircraft are delivered to the airspace in the same amount of time and keeping all aircraft on their planned routes becomes more difficult.

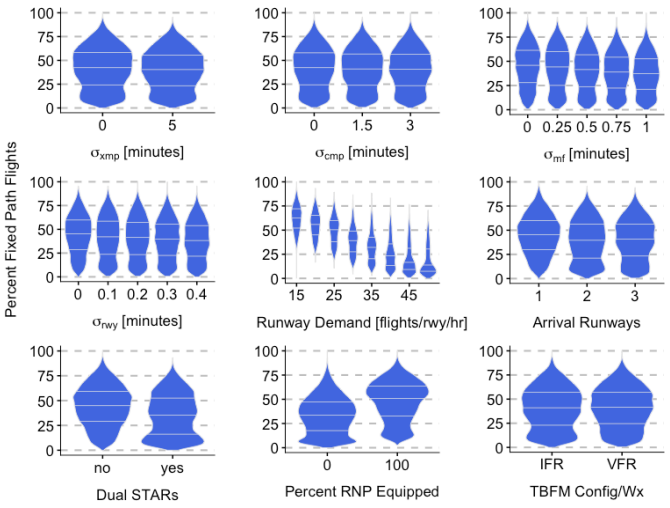

Figure 9. Marginal Effects of Inputs on the Percent of Fixed Path Flights

The next most influential input is the RNP equipage. The violin plots show that very high and very low percentages of flights can fly fixed paths with either simulated setting (0% and 100% equipped). However, three quarters of simulations with no RNP equipage result in fewer than 50% of aircraft flying fixed paths, while more than half of simulations with full RNP equipage result in greater than 50% of aircraft flying fixed paths. This is, in part, due to the qualitative difference between flying a fixed TBFM route and flying an RNP approach. TBFM routes are less constrained than RNP approaches and therefore allow for more delay to be absorbed before a re-route is necessary. Re-routing an aircraft off an RNP approach is not a complicated task in either the real operation or in the simulated one, but in both cases, there is a higher decision threshold and more effort is made to absorb the delay further upstream. Additionally, RNP approaches, while affording less delay authority than TBFM-assumed fixed path approaches, also provide more consistent traversal times across aircraft types.

The other seven input values do not seem to have a strong impact on the percent of fixed path flights in a simulation independent of other variable settings. Most of them stretch from close to 0% fixed path flights to near 100% fixed path flights. However, the results are more nuanced. The effect of large delivery errors to the XMP depends on the delivery errors to the CMP and MF, the number of arrival runways, and so on.

To better understand the trade space between input variables and the percentage of flights that can fly fixed paths uninterrupted, a fractional response regression model [14] [15] was fit to the simulation results, as shown in equation (1). A fractional response model is like logistic regression but allows for response variables on the interval [0, 1] instead of requiring a binomial response of either 0 or 1.

$$
\begin{aligned}
&\ln\left(\frac{\hat{\theta}(\sigma,X)}{1-\hat{\theta}(\sigma,X)}\right) = 0.971 - 0.048\sigma_{XMP} - 0.032\sigma_{CMP} - \\
&0.732\sigma_{MF} - 1.27\sigma_{RWY} - 0.3x_{\text{rwy demand}} + \\
&0.343x_{\text{is RNP}} + 0.378x_{\text{dual STARs}} - 0.107x_{\text{n rwys}} - \\
&0.054x_{\text{VMC}} + 0.01(\sigma_{XMP})(\sigma_{MF}) + 0.017(\sigma_{XMP})(\sigma_{RWY}) + \\
&0.005(\sigma_{XMP})(x_{\text{rwy demand}}) + 0.007(\sigma_{XMP})(x_{\text{n rwys}}) + \\
&0.01(\sigma_{CMP})(\sigma_{MF}) - 0.011(\sigma_{CMP})(x_{\text{dual STARs}}) + \\
&0.011(\sigma_{CMP})(x_{\text{n rwys}}) + 0.59(\sigma_{MF})(\sigma_{RWY}) + \\
&0.049(\sigma_{MF})(x_{\text{rwy demand}}) + 0.129(\sigma_{MF})(x_{\text{is RNP}}) - \\
&0.128(\sigma_{MF})(x_{\text{dual STARs}}) + 0.044(\sigma_{MF})(x_{\text{n rwys}}) + \\
&0.046(\sigma_{RWY})(x_{\text{rwy demand}}) + 0.438(\sigma_{RWY})(x_{\text{is RNP}}) - \\
&0.313(\sigma_{RWY})(x_{\text{dual STARs}}) - 0.175(x_{\text{rwy demand}})(x_{\text{dual STARs}}) + \\
&0.017(x_{\text{rwy demand}})(x_{\text{VMC}}) + 0.145(x_{\text{is RNP}})(x_{\text{dual STARs}}) + \\
&0.12(x_{\text{is RNP}})(x_{\text{n rwys}}) - 0.191(x_{\text{dual STARs}})(x_{\text{n rwys}}) + \\
&0.023(x_{\text{dual STARs}})(x_{\text{VMC}}) + 0.024(x_{\text{n rwys}})(x_{\text{VMC}})
\end{aligned}
\tag{1}
$$

In this model $\theta(\sigma, X)$ is the proportion of flights that are expected to fly a fixed path. For a particular set of operational characteristics, x, and target delivery accuracies, σ, the entire right-hand side of the equation reduces to some number y. From there, the expected proportion of success is given by:

$$\hat{\theta}(\sigma, X) = \frac{e^y}{1+e^y} \tag{2}$$

The model terms on the right-hand side are defined as follows:

- σ_{XMP} represents the standard deviation of delivery error (in minutes) for a Normal distribution (with mean at zero) governing the errors used by the simulation when delivering flights to the XMP. σ_{CMP}, σ_{MF}, and σ_{RWY} are defined similarly for the CMP, MF, and at TMPs inside the TRACON, respectively.
- $x_{\text{rwy demand}}$ captures the runway demand starting at 15 flights/runway/hour and specified in 5-flight/runway/hour increments. For example, $x_{\text{rwy demand}} = 0$ represents a demand of 15 flights/runway/hour and $x_{\text{rwy demand}} = 4$ represents a demand of (5•4)+15=35 flights/runway/hour.

Although somewhat counterintuitive, this convention helps simplify the interpretation of model coefficients.

- $x_{\text{is RNP}}$ is an indicator variable that takes a value of 1 if the simulation was run with 100% RNP-equipped aircraft and 0 if the simulation was run with no RNP-equipped aircraft. The RNP equipage rate was treated as a qualitative variable instead of a continuous variable because no simulations were run in a mixed-equipage environment. Given this constraint on the data from which the regression model was derived, it is not appropriate to try to use this model to predict PBN utilization in mixed-equipage operations, where some flights are RNP-equipped and some are not.
- $x_{\text{dual STARS}}$ is an indicator variable that takes a value of 1 if dual STARs per corner post were used and 0 otherwise.
- $x_{\text{n rwys}}$ reports the number of arrival runways in excess of 1. Thus, $x_{\text{n rwys}} = 0$ represents a one-runway operation, $x_{\text{n rwys}} = 1$ represents a two-runway operation, and $x_{\text{n rwys}} = 2$ represents a three-runway operation.
- x_{VMC} is an indicator variable that takes a value of 1 for VMC and 0 for IMC.

Figure 10 illustrates the application of the regression model and compares regression model predictions with simulation results. In this figure, all simulations are shown where $\sigma_{XMP} = \sigma_{CMP} = \sigma_{MF} = \sigma_{RWY} = 0$. The boxplots in the background summarize the simulated results. The blue points (with randomized locations over the width of the boxplot for better visibility) are predicted using the regression model. The blue curve across the plot is a non-parametric best fit line through the predicted points. The key observation here is for these cases with perfect delivery accuracy, the regression model is quite good at predicting the percentage of fixed path flights. Note that the best-fit curve (based on regression model predictions) passes near the middle of most of the boxplots (based on simulation results). However, the agreement between the regression model and the simulation results (again for perfect delivery errors) degrades somewhat as runway demand exceeds 35 flights per runway per hour when delivery errors are at their extreme values. Most model-predicted values for a demand of 50 flights/runway/hour are below the median simulated value.

Figure 11 is similar to Figure 10, except that in this case only simulations with large delivery errors were used ($\sigma_{XMP} = 5$ min, $\sigma_{CMP} = 5$ min, $\sigma_{MF} = 1$ min, and $\sigma_{RWY} = 24$ s) to construct the background boxplots and the regression model was used to predict the percent of fixed path flights in these situations. This figure shows that the regression model provides reasonable agreement with the model when delivery errors are large in addition to agreeing well with the simulation results in cases with perfect delivery.

Given that the regression model has been shown to represent the behavior of the simulation, it may be used to better understand how different input settings impact the resulting fixed path rate. The effect of each input variable is described in more detail below.

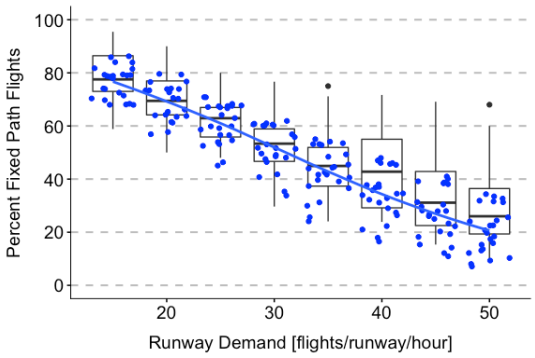

Figure 10. Comparison of Regression Model Predictions and Simulation Results for Small Delivery Errors

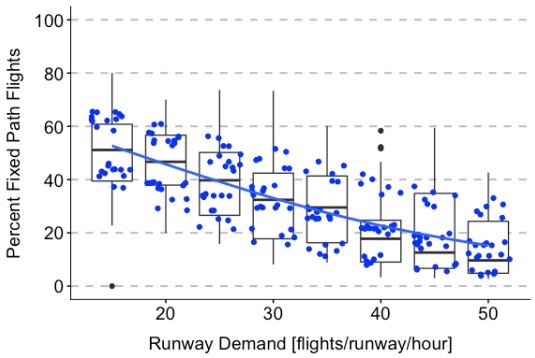

Figure 11. Comparison of Regression Model Predictions and Simulation Results for Large Delivery Errors

A. *Effect of Delivery Error at MRPs*

Equation (3) represents the model simplified by setting all operational characteristics to zero. This isolates those terms in the regression model that involve only delivery errors at each of the MRPs (σ). It is important to recall that there are other interaction effects involving delivery errors and other features of an operation that are omitted here for simplification.

$$\begin{aligned}\ln\left(\frac{\hat{\theta}(\sigma,X)}{1-\hat{\theta}(\sigma,X)}\right) =& 0.971 - 0.048\sigma_{XMP} - 0.032\sigma_{CMP} \\ &- 0.732\sigma_{MF} - 1.27\sigma_{RWY} \\ &+ 0.01(\sigma_{XMP})(\sigma_{MF}) \\ &+ 0.017(\sigma_{XMP})(\sigma_{RWY}) \\ &+ 0.01(\sigma_{CMP})(\sigma_{MF}) \\ &+ 0.59(\sigma_{MF})(\sigma_{RWY})\end{aligned} \tag{3}$$

Increasing errors inside the TRACON is most detrimental to promoting fixed path flights (that coefficient is the biggest in absolute value). After that, increasing errors at the MF, XMP, and CMP have, in that order, the most detrimental effect on the percentage of fixed flight paths. Taking a simple case, where $\sigma_{CMP} = \sigma_{MF} = \sigma_{RWY} = 0$, then the effect of increasing σ_{XMP} from 0 minutes to 1 minute, is given by (4).

$$\hat{\theta}(\sigma, X) = \frac{e^{-0.048*1}}{1+e^{-0.048*1}} - \frac{e^{-0.048*0}}{1+e^{-0.048*0}} = -0.012 \quad (4)$$

This means that the model estimates the increased error will decrease the proportion of fixed path flights by 1.2 percentage points (assuming zero delivery error at the CMP, MF, and inside the TRACON). In other words, if 80% of aircraft were flying fixed paths when $\sigma_{XMP}=0$, but then σ_{XMP} is increased to 1 minute (i.e., roughly delivering aircraft within two minutes of the STA) without changing any other factors, the model would expect 78.8% of aircraft to fly a fixed path.

A decrease of 1.2 percentage points is modest. The effect of an isolated increase in delivery error at the CMP (again from 0 minutes to 1 minute) is even less, decreasing the expected percent of aircraft flying fixed paths by 0.8 percentage points. The effect of similar increases in error at the MF and inside the TRACON are much more pronounced, with the model expecting 18 and 28 percentage point decreases in the fixed path rate, respectively, if errors are increased from 0 minutes to 1 minute, holding all other variables constant.

Turning to the relationships between delivery errors, consider the interaction between delivery errors at the MF and inside the TRACON, shown in Figure 12. When there are no delivery errors to either the MF or inside the TRACON (the far-left point of the green curve) the result is that the expected proportion of fixed path flights is not adjusted down at all. If all other variables were also zero, the model predicts 73% of flights will fly a fixed path.

Holding error inside the TRACON constant, increasing the error at the MF has clear negative effects. For example, increasing σ_{MF} from 0 to 30 seconds would cause the estimated fixed path rate to drop nearly 10 percentage points, all other variables being held constant. Similarly, if error at the MF is held constant, the negative slopes of each of the curves show that larger errors in the TRACON correspond to lower fixed path rate predictions.

The interesting thing about this plot, however, is that as both errors increase, the overall effect on fixed path rates remains negative, but the magnitude of the effect diminishes. Consider how the green and orange curves are separated by nearly 10 percentage points at the far-left side of the plot (where $\sigma_{RWY}=0$) but are only separated by about 5 percentage points at the far right (where $\sigma_{RWY}=30$ seconds). This mitigation effect is caused by the interaction term in (3). The positive sign of the coefficient reduces the overall negative effect corresponding to increasing errors individually. Notably, though all main effects are negative (increasing error is bad for fixed path flights) all interaction terms are positive (so the negative effects are not quite additive).

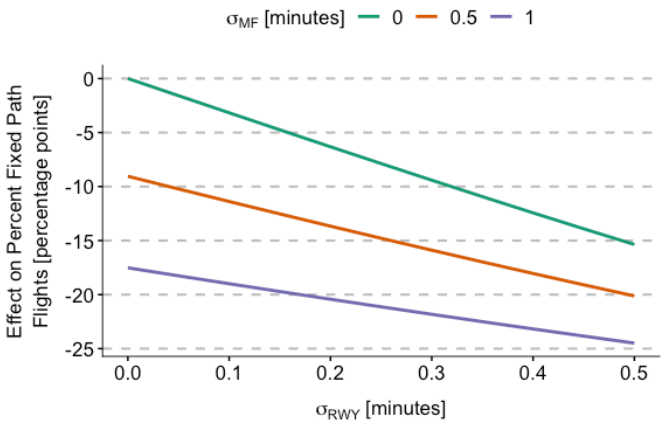

Figure 12. Interaction between Delivery Errors at the MF and Inside the TRACON

B. *Effect of Runway Demand*

Increasing runway demand will, in isolation, decrease the model-predicted fixed path rate. However, this term interacts with all input variables except σ_{CMP}. The terms in (3) involving runway demand have been extracted from the regression model (1). Other terms are relegated to the catch-all constant *C*. For example, (3) includes the interaction between σ_{XMP} and $x_{\text{rwy demand}}$ but here the focus is not on the main effect of σ_{XMP} since that was already discussed. Thus, the main effect term for error at the XMP is captured in *C* to simplify things.

$$\begin{aligned}\ln\left(\frac{\hat{\theta}(\sigma,X)}{1-\hat{\theta}(\sigma,X)}\right) = &-0.3x_{\text{rwy demand}} \\ &+0.005(\sigma_{XMP})(x_{\text{rwy demand}}) \\ &+0.049(\sigma_{MF})(x_{\text{rwy demand}}) \\ &+0.046(\sigma_{RWY})(x_{\text{rwy demand}}) \\ &-0.175(x_{\text{rwy demand}})(x_{\text{dual STARs}}) \\ &+0.017(x_{\text{rwy demand}})(x_{\text{VMC}})+C\end{aligned} \quad (5)$$

When all other inputs are at their zero-values (i.e., all interaction terms are zeroed out), then increasing $x_{\text{rwy demand}}$ from 0 (representing 15 flights/runway/hour) to 1 (representing 20 flights/runway/hour) reduces the probability of a flight flying a fixed path by about 7.4 percentage points. This means it becomes more difficult to support fixed path arrivals as demand increases.

Each of the coefficients on interaction terms involving one of the delivery accuracy inputs is positive, meaning that if runway demand is increased and delivery errors at the XMP, MF, and/or inside the TRACON also increased, the overall negative effect of increased runway demand is lessened, similar to what was observed with Figure 12. However, because the main effects of σ_{XMP}, σ_{MF}, and σ_{RWY} are all negative, when delivery errors and runway demand increase simultaneously, the positive interaction terms are outweighed by the negative main effects and the overall impact on the fixed path rate is negative.

Visual weather conditions help mitigate the negative effect of increasing runway demand on the rate of fixed path flights, but dual STARs have the opposite effect. Holding all other variables at their zero-values, for example, increasing $x_{\text{rwy demand}}$ from 15 to 20 flights/runway/hour reduces the expected fixed path rate by 7.4 percentage points as noted above. Given a scenario that is the same in every respect except that dual STARs are used, the expected fixed path rate would be decreased by 11.7 percentage points. The impact of Dual STARs is further explored below.

C. *Effect of RNP Equipage*

The effect of RNP equipage on fixed path flights is purely positive. Equation (6) isolates the related terms from the regression model (1).

$$\begin{aligned}\ln\left(\frac{\hat{\theta}(\sigma,X)}{1-\hat{\theta}(\sigma,X)}\right) =& 0.343x_{\text{is RNP}} \\ &+ 0.129(\sigma_{MF})(x_{\text{is RNP}}) \\ &+ 0.438(\sigma_{RWY})(x_{\text{is RNP}}) \\ &+ 0.145(x_{\text{is RNP}})(x_{\text{dual STARs}}) \\ &+ 0.12(x_{\text{is RNP}})(x_{\text{n rwys}}) + C\end{aligned} \tag{6}$$

Not only does the main effect term ($0.343x_{\text{isRNP}}$) have a positive coefficient, but every interaction term has a positive coefficient. This means that $x_{\text{isRNP}} = 1$ (i.e., full RNP equipage instead of no RNP equipage) will help any scenario improve. The main effect improvement (before considering any interactions) is to increase the chance of a fixed path flight by about 8.5 percentage points. The interaction terms help to partially mitigate the negative effects of increasing errors at MRPs and increasing runways.

D. *Effect of Dual STARs*

Equation (7) isolates terms involving dual STARs.

$$\begin{aligned}\ln\left(\frac{\hat{\theta}(\sigma,X)}{1-\hat{\theta}(\sigma,X)}\right) =& 0.378x_{\text{dual STARs}} \\ &- 0.011(\sigma_{CMP})(x_{\text{dual STARs}}) \\ &- 0.128(\sigma_{MF})(x_{\text{dual STARs}}) \\ &- 0.313(\sigma_{RWY})(x_{\text{dual STARs}}) \\ &- 0.175(x_{\text{rwy demand}})(x_{\text{dual STARs}}) \\ &+ 0.145(x_{\text{is RNP}})(x_{\text{dual STARs}}) \\ &- 0.191(x_{\text{dual STARs}})(x_{\text{n rwys}}) \\ &+ 0.023(x_{\text{dual STARs}})(x_{\text{VMC}}) + C\end{aligned} \tag{7}$$

The role that dual STARs have in exacerbating the negative effect of increasing runway demand has already been discussed. Interestingly, however, the main effect of dual STARs is positive. If all interaction terms were zero and all other variables held constant, then moving from a single STAR operation to using dual STARs is expected to increase the fixed path rate by 9.3 percentage points. However, due to the way dual STARs interact with other variables, having them can be detrimental in some situations. This is illustrated by Figure 13.

Considering only dual STARs and runway demand (the left plot), when $x_{\text{rwy demand}} = 0$ (i.e., 15 flights/runway/hour) the interaction term is zero, the main effect of dual STARs is positive, and therefore, the presence of dual STARs is expected to increase the percent flights flying a fixed path by close to 10 percentage points. However, the combined effect of increasing runway demand and the interaction with dual STARs makes the orange line slope down more steeply, such that dual STARs are still helpful at a demand of 25 flights/runway/hour, but detrimental for higher runway demands.

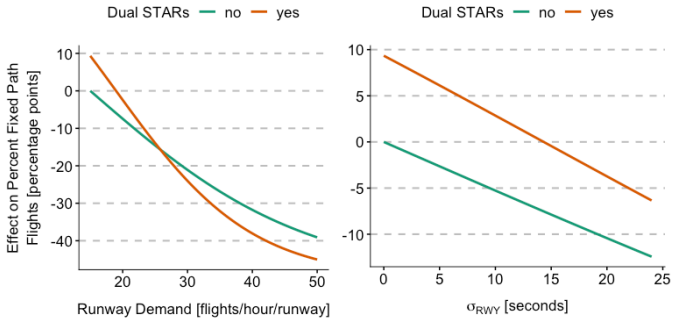

Figure 13. Dual STARs Interacting with Runway Demand and TRACON Errors

The right plot in Figure 13 shows that over the range of simulated runway delivery errors in the TRACON (with all other variables at their zero-levels), the use of dual STARs helps increase the expected percentage of fixed path flights. The positive main effect of dual STARs offsets the orange line above the green, but the slope of the orange is a bit steeper with respect to σ_{RWY}.

It is important to recall that the above results are predicated upon other variables being at their zero-values. In addition to depending on the delivery error inside the TRACON and runway demand, the effect of dual STARs also depends on delivery errors at the CMP and MF, as well as the number of runways, RNP equipage, and weather conditions.

E. *Effects of Other Input Variables*

Other predictor variables incclude the number of runways ($x_{\text{n rwys}}$) and the weather conditions (x_{VMC}). Somewhat counterintuitively the main effect of increasing the number of runways was a small decrease in the expected fixed path rate. This results primarily from how the variable was coded, since increasing the number of runways actually increases the total traffic in a simulation if the runway demand (per runway) is held constant. There was also a small negative effect assoicated with VMC conditions that may be the result of shorter paths with less distance over which to absorb delay.

VI. Conclusions

This paper presented a fast-time simulation model of a time-based metering operation to study the impact of operational characteristics and delivery accuracy on the percentage of flights that remain on their planned path throughout the arrival and approach operation. The simulation output was the percentage of flights that adhered to a fixed path from initiation until the runway, meaning those flights that conformed to both the STAR and the planned approach path.

A fractional response regression model was derived from the results of the fast-time simulation. This regression model was used to estimate the percentage of fixed path flights given different operational characteristics and assumed delivery accuracy performance. While the regression model was derived using a model and simulation results for KDEN, the model may be applied to other sites to determine delivery accuracy performance requirements to achieve the desired fixed path percentage by setting the operational characteristics to represent the site of interest.

The regression model can also be used to understand the complex relationships between operational characteristics and metering performance on fixed path. One key insight is runway demand, defined as the number of flights per runway per hour, had the largest impact on the percentage of flights that flew fixed paths, but the size of the impact decreased as the runway demand increased. Up to 35 flights/runway/hour, increasing the demand by 5 flights/runway/hour causes the rate of fixed path arrivals to drop by about 7 percentage points, all other variables held constant, but at higher demand levels the effect is smaller. As runway demand increased, more tactical interventions were needed with more flights being vectored or re-routed to ensure separation. RNP equipage also had a significant impact on the percentage of flights remaining on fixed paths. Comparing cases where 100% of flights were RNP-equipped or zero flights were RNP-equipped, the fixed path rate increased by 9 percentage points, holding all other variables constant, when aircraft were RNP equipped. This followed from greater predictability and redistribution of delay upstream of the RNP approaches.

Increasing delivery errors was detrimental to fixed path rates. Increasing errors inside the TRACON had the largest negative effect followed by the MF, XMP, and CMP. Holding all other variables constant, increasing individual delivery errors from zero to roughly ±2 min (σ = 1 min) inside the TRACON, at the MF, at the CMP, and at the XMP decreased the fixed path rate of the resulting operation by 28.0, 17.5, 0.8, and 1.2 percentage points, respectively. These results reflect increasing one delivery error at a time, not all at once.

REFERENCES

[1] Federal Aviation Administration, “Trajectory-based Operations (TBO) 2025 Vision," Tech. rep., Washington, DC, 2017; https://my.faa.gov/org/staffoffices/ang/reports_plans.html.

[2] Federal Aviation Administration, “Performance Based Navigation (PBN) NAS Navigation Strategy 2016,” Technical Report, Washington, DC, 2016.

[3] Federal Aviation Administration, “TBFM Animated Storyboard,” URL:https://www.faa.gov/about/office_org/headquarters_offices/ang/offices/tc/library/Storyboard/detailedwebpages/tbfm.html.

[4] Gregory Wong, “The Dynamic Planner: The Sequencer, Scheduler, and Runway Allocator for Air Traffic Control Automation,” NASA Technical Report, NASA/TM-2000-209586, April 2000.

[5] Brock Lascara, Lesley Weitz, Tom Monson, and Robert Mount, “Measuring Performance of Initial Ground-based Interval Management – Spacing (GIM-S) Operations,” in the proceedings of the USA/Europe Air Traffic Management Research & Development Seminar, 2017.

[6] Michael Kupfer, Todd Callantine, Lynne Martin, Joey Mercer, and Everett Palmer, “Controller Support Tools for Schedule-Based Terminal-Area Operations,” in the proceedings of the USA/Europe Air Traffic Management Research & Development Seminar, 2011.

[7] Jane Thipphavong, Jaewoo Jung, Harry Swenson, Lynne Martin, Melody Lin, and Jimmy Nguyen, “Evaluation of the Terminal Sequencing and Spacing System for Performance-based Navigation Arrivals,” in the proceedings of the Digital Avionics Systems Conference, 2013.

[8] Kevin Witzberger and Lynne Martin, “Paradigm Changes Related to TSAS: Viewed Through the Perspective of the FAA/NASA Operational Integration Assessment,” ATCA Journal, Winter 2015.

[9] I. M. Levitt, L. A. Weitz, and M. W. Castle, “Modeling Delivery Accuracy for Metering Operations to Support RNAV Arrivals,” Tenth USA/Europe Air Traffic Management Research and Development Seminar (ATM2013), Chicago, Illinois, 2013.

[10] S. Shresta and R. H. Mayer, “Benefits and Constraints of Time-Based Metering Along RNAV STAR Rotues,” 28th Digital Avionics Systems Conference (DASC), Orlando, Flordia, 2009.

[11] S. Shresta and R. H. Mayer, “Modeling of Air Traffic Arrival Operations through Agent-Based Simulation,” Proceedings of the 2008 Winter Simulation Conference, Miami, Flordia, 2008

[12] The Federal Aviation Administration, D01, and DEN Air Traffic Control Tower (ATCT), “Waiver to FAA Order JO 7110.65 Paragraph 59-11a1, Simultaneous Independent Approaches to Widely Spaced Parallel Runways without Final Monitors; Denver TRACON/Denver International Airport ATCT Safety Risk Management Document,” Denver, Colorado, 2014

[13] The Federal Aviation Administration, “Memorandum: Required Navigation Performance Authorization Required Curved Path Approaches to Widely Spaced Runways,” Washington, D.C., 2014.

[14] L. E. Papke and J. M. Wooldridge, “Econometric Methods for Factional Response Variables with an Application to 401(K) Plan Participation Rates,” Journal of Applied Economics, vol. 11, pp. 619-632, 1996.

[15] S. J. Sheather, “A Modern Approach to Regression with R,” Springer, 2009.

This work was produced for the U.S. Government under Contract DTFAWA-10-C-00080 and is subject to Federal Aviation Administration Acquisition Management System Clause 3.5-13, Rights In Data-General, Alt. III and Alt. IV (Oct. 1996).